Pre-print version (generated on 15.12.2021)
This and other publications are available at:
http://www.acin.tuwien.ac.at/publikationen/ams/

High-bandwidth tip-tilt vibration compensation in telescope systems ⋆

Andreas Sinn, Thomas Riel, Florian Deisl, Stephan Schachner, Georg Schitter

Automation and Control Institute, TU Wien, 1040 Vienna, Austria (e-mail: sinn@acin.tuwien.ac.at).

Abstract: Mechanical vibrations resulting from wind, ground vibrations and actuator imperfections lower the performance of optical telescope systems used for astronomical applications, as well as free-space optical communication. This paper proposes a high-bandwidth tip-tilt compensation system for optical telescopes, in order to reduce the influence of these vibrations. A typical, high precision, motorized telescope system is used as a base for this evaluation. By utilization of a tip-tilt sensor, the resulting tip-tilt errors are measured and analyzed in the frequency domain. A fast steering mirror integrated into the optical path allows to compensate for the measured tip-tilt errors. The performance of the fast steering mirror based system is compared to the original, uncompensated system, as well as to a compensation loop, which uses the telescope mount to counteract measured errors. Experiments demonstrate a significant reduction of the tip-tilt errors due to vibrations by a factor of 5 (altitude axis) and by a factor of 4.6 (azimuth axis) utilizing a compensation bandwidth of up to 810 Hz.

Keywords: Vibration compensation, telescopes, optical communication, fast steering mirror, tip-tilt compensation

1. INTRODUCTION

Modern, high-precision telescope systems are used for a variety of applications ranging from Astronomy, over space debris observation to free-space optical (FSO) satellite communication. All those applications require precise and steady pointing even at tracking speeds faster than sidereal (earth rotation velocity) tracking. Typical systems target a pointing precision below 1 µrad [Hemmati (2007)]. Mechanical vibrations due to ground vibrations, wind-shake and the telescope mount actuators itself cause mainly tip-tilt aberrations and limit the achievable precision of these systems [Hardy (1998); Bely (2003)]. Furthermore, these vibrations may not be observed by the encoders of the telescope mount actuators. A commonly used approach for telescope systems is the use of feed-forward vibration compensation based on accelerometer measurements [Lee et al. (2001); Keck et al. (2014); Glück et al. (2017)]. In combination with a fast steering mirror (FSM) fast compensation of vibrations is possible. However, sensor placement is crucial and structural modes of the telescope tube may not be observable. Therefor, a system which takes the influence of vibrations onto the optical path into account, is necessary.

An optical tip-tilt sensor (e.g. quad photo diode, position sensitive device [Kaymak et al. (2018)]) serves as source, providing an absolute measurement of the telescope's pose. The contributions of all mentioned error sources acting onto the system are observable with this sensor. Furthermore, the resulting tip-tilt aberrations due to atmospheric turbulence are covered too. While tip-tilt compensation using FSMs or actuated secondary mirrors, is quite common for classical astronomical applications with large telescope diameters (greater than 2 m) [Pickles et al. (1994); Jim et al. (2000); Peter et al. (2012)], small telescope systems (less than 1 m aperture), which have become popular over the last decade, usually lack this kind of compensation systems. In Riesing et al. (2017) a compensation system based on a camera and a FSM was used for development of a low-cost optical ground-station with a bandwidth below 10 Hz. Sinn et al. (2019) present tip-tilt compensation for atmospheric turbulence with a 35 cm telescope and a bandwidth of 550 Hz. Also the application guiding and vibration compensation in airplane-to-ground links has been studied [Schmidt (2012)].

However, the applicability and possible potential of compensating vibrations using the mount actuators of small telescopes has not been evaluated in detail. Furthermore, the increasing demands towards stabilized, high-performance platforms for FSO and space debris observation using small telescopes, necessitate the availability of high-bandwidth tip-tilt compensation systems, with minimized susceptibility to vibrations and also other disturbance sources, such as atmospheric turbulence.

This paper proposes a high-bandwidth tip-tilt compensation for vibration suppression on a small telescope system. The system consists of a FSM and a quad-photo diode (QPD) mounted on top of a state of the art, high-precision telescope mount. The sensor information from the QPD is used to measure present tip-tilt errors in the system and compensate for them by means of the FSM in closed loop

⋆ This work was funded by the Austrian Ministry for Transport, Innovation and Technology (BMVIT) under the scope of the Austrian Space Applications Program (FFG project number 854050).

Pre-print version of the article: A. Sinn, T. Riel, F. Deisl, S. Schachner, and G. Schitter, "High-bandwidth tip-tilt vibration compensation in telescope systems," *Joint Conference 8th IFAC Symposium on Mechatronic Systems (MECHATRONICS 2019),* vol. 52, no. 15, pp. 549 – 554, 2019. DOI: 10.1016/j.ifacol.2019.11.733
© 2019. This manuscript version is made available under the CC-BY-NC-ND 4.0 license
http://creativecommons.org/licenses/by-nc-nd/4.0/

Pre-print version (generated on 15.12.2021)
This and other publications are available at:
http://www.acin.tuwien.ac.at/publikationen/ams/

operation. Furthermore, the sensor information is used for comparison in a closed loop system with the telescope mount. The paper's main contribution is the comparison of both compensation loops to the original system and the evaluation of their performance gain in a laboratory environment. Additionally, the proposed system allows compensation of the influence of atmospheric turbulence and pointing uncertainties, because it measures the resulting tip-tilt aberrations.

The remaining paper is organized as follows. Section 2 gives an overview of the used system components. In Section 3 the system dynamics are identified and corresponding controllers are designed. In Section 4 the measurement results without and with control are discussed and Section 5 provides conclusion and outlook.

2. SYSTEM DESCRIPTION

The investigated system as shown in Figure 2 is based on a high-precision, direct-drive telescope mount (DDM60, ASA Astrosysteme GmbH, Neumarkt, Austria) with custom made motor controllers optimized for high tracking speed and precision [Riel et al. (2018a,b)]. Riel et al. (2017) investigate this mount in a vibration isolated environment, demonstrating a position error below 300 nrad RMS at a tracking rate of up to 1 dps. In this publication the system is mounted on top of a mobile workbench, with retractable wheels and operated in typical laboratory environment without vibration isolation.

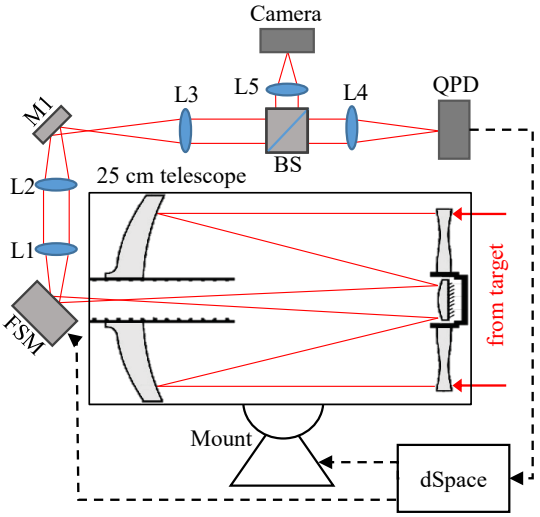

Fig. 1. System architecture of the proposed vibration compensation system.

The optical system is built around a 10 inch Schmidt-Cassegrain telescope with a focal length of 2.54 m. A schematic overview of this system is given in Figure 1. A commercial FSM (OIM101, Optics in Motion, Long Beach, USA) with a diameter of 1 inch is mounted instead of the tertiary mirror and directs the received light towards an optical breadboard mounted on top of the telescope. This FSM provides a mechanical actuation range of ±26.2 mrad, and its axes are aligned with the altitude (alt)

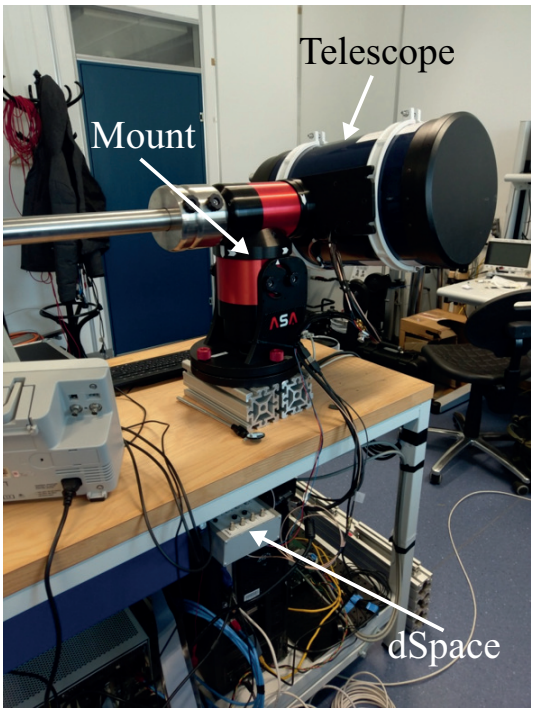

Fig. 2. Image of the investigated system showing the telescope system and the workbench.

and azimuth (az) axes of the telescope mount. The FSM is driven by custom made, analog PI current controllers (based on OPA549TG, Texas Instruments, Dallas, USA). A 50:50 beam splitter (Thorlabs CM1-BS013) is used to guide the incident light to a QPD circuit (based on S5980, Hamamatsu, Hamamatsu, Japan) on a PCB with integrating summing and subtraction amplifiers. A camera (ASI 290 MM Mono, ZWO Company, Suzhou, China), is installed for alignment purpose.

As the reference target, a custom made artificial star based on a LED with a center wavelength of 630 nm and an aperture diameter of 50 µm is used. The measurement distance between telescope and artificial star is approximately 18 m. Signal acquisition and feedback control are implemented on a dSpace rapid prototyping system (DS1202, dSpace GmbH, Germany). A sampling frequency of 18 kHz is used. The mount is connected to the dSpace system over a serial interface connection with a Baud rate of 230400 Baud, which allows an update rate significantly higher than the bandwidth of interest.

3. SYSTEM IDENTIFICATION AND CONTROLLER DESIGN

In order to identify the system dynamics a system analyzer (HP 3562A, Hewlett-Packard, CA, USA) is utilized. The telescope is statically pointing at the artificial star. The center of the QPD is aligned to the focused spot of the star, providing altitude and azimuth position information for all measurements.

Pre-print version of the article: A. Sinn, T. Riel, F. Deisl, S. Schachner, and G. Schitter, "High-bandwidth tip-tilt vibration compensation in telescope systems," *Joint Conference 8th IFAC Symposium on Mechatronic Systems (MECHATRONICS 2019),* vol. 52, no. 15, pp. 549 – 554, 2019. DOI: 10.1016/j.ifacol.2019.11.733
© 2019. This manuscript version is made available under the CC-BY-NC-ND 4.0 license
http://creativecommons.org/licenses/by-nc-nd/4.0/

Pre-print version (generated on 15.12.2021)
This and other publications are available at:
http://www.acin.tuwien.ac.at/publikationen/ams/

3.1 Telescope mount

To measure the frequency response of the telescope mount, its external inputs for the desired position of both axes are used. The mount, the optical system and the QPD are considered as plant for this measurement (Figure 3). The FSM is controlled to zero angular deflection by means of an integrated controller, behaving as fixed tertiary mirror. In Figures 4 and 5 these frequency responses are shown for the altitude axis and the azimuth axis, respectively. The -3 dB bandwidth of 5.6 Hz for the azimuth and 13.5 Hz for the altitude axis is given by the integrated controllers of the mount. These parameters, as well as several notch filters are chosen automatically during a tuning and calibration procedure and are not further investigated in this publication [Riel et al. (2018a)]. The impact of these (to some extend overcompensating) notch filters can be seen at 27 Hz and 210 Hz (altitude axis) and 42 Hz (azimuth axis). Besides this information the mount is considered as a black box.

For bandwidth maximization the cascaded control loop (Figure 3) could be reduced to a single, QPD feedback based loop. However, this would result in a loss of (blind) trajectory tracking capabilities, which is undesired for the named applications.

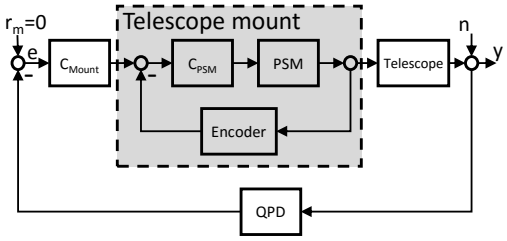

Fig. 3. Block diagram for one axis of the designed QPD based feedback controller (C_{Mount}), which uses the telescope mount as actuator, where n is the output disturbance. The telescope mount's internal control structure is also shown. r_m is the reference input which is set to zero.

Based on the measured plant dynamics of the mount, PID controllers are designed. Due to the fact that the magnitude of the crosstalk between both mount axes is below 20 dB for the relevant frequency range, the motion of the altitude and azimuth axes are considered independent and therefor, the design of an independent SISO controller for each axis is justified. For the design, plant models are derived based on the measured frequency responses by using the MATLAB `fitsys` algorithm and are shown in Figures 4 and 5 [Yamaguchi et al. (2011)]. Tamed PID controllers in parallel structure are designed based on the plant model [Munning Schmidt et al. (2014)]. Their basic transfer function is given by

$$C_{\text{Mount}}(s) = K_p + \frac{K_i}{s} + \frac{K_d s}{\tau_t s + 1}, \tag{1}$$

with K_p as proportional, K_i as integral and K_d as derivative controller gains. A filter with the time constant τ_t limits the differentiating behavior at high frequencies. The

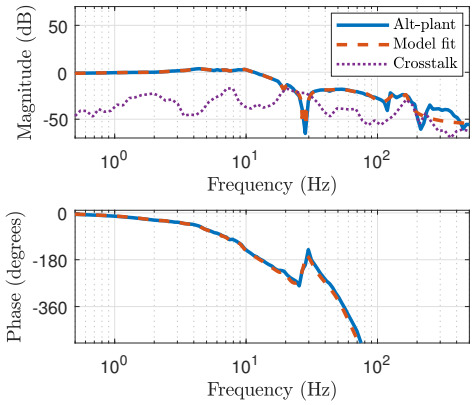

Fig. 4. Frequency response of the altitude axis of the mount and the corresponding fit model. The magnitude of the measured crosstalk (dashed yellow) between the two axes is about 25 dB below the single axis response.

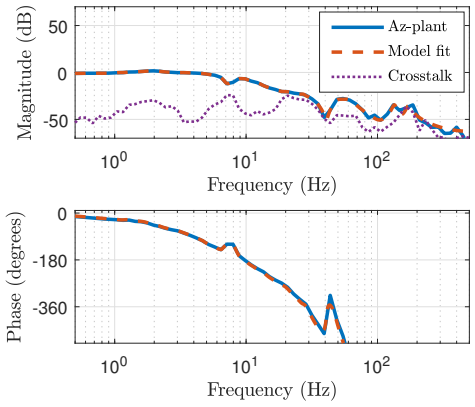

Fig. 5. Frequency response of the azimuth axis of the mount and its model fit. The magnitude of the measured crosstalk (dashed yellow) between the two axes is about 30 dB below the single axis response.

unity-gain crossover frequency is set to 1.25 Hz for the alt-axis and 0.57 Hz for the az-axis, which effectively results in PI-controllers with a closed loop bandwidth of 3.1 Hz (alt) and 0.8 Hz (az). As these gains are tuned for maximum bandwidth, an inherent limitation given by the mount and its actuators is visible. Due to the large moving mass of the telescope and the corresponding moment of inertia, in combination with restricted actuator torque, the maximal achievable bandwidth is limited.

3.2 Fast steering mirror

To overcome the limitations of achievable compensation bandwidth given by the dynamic behavior of the mount, the FSM is used (Figure 6). The frequency response of the FSM plant consisting of the power amplifiers, the FSM, the optical setup and the QPD is shown in Figure 7. At

Pre-print version of the article: A. Sinn, T. Riel, F. Deisl, S. Schachner, and G. Schitter, "High-bandwidth tip-tilt vibration compensation in telescope systems," *Joint Conference 8th IFAC Symposium on Mechatronic Systems (MECHATRONICS 2019),* vol. 52, no. 15, pp. 549 – 554, 2019. DOI: 10.1016/j.ifacol.2019.11.733
© 2019. This manuscript version is made available under the CC-BY-NC-ND 4.0 license
http://creativecommons.org/licenses/by-nc-nd/4.0/

Pre-print version (generated on 15.12.2021)
This and other publications are available at:
http://www.acin.tuwien.ac.at/publikationen/ams/

low frequencies both axes show typical behavior of spring-damper-mass system, with the suspension mode of the mirror located at 27 Hz. At frequencies above 1 kHz a second resonance peak is visible in both axes, which is caused by the second eigenmode of the mirror.

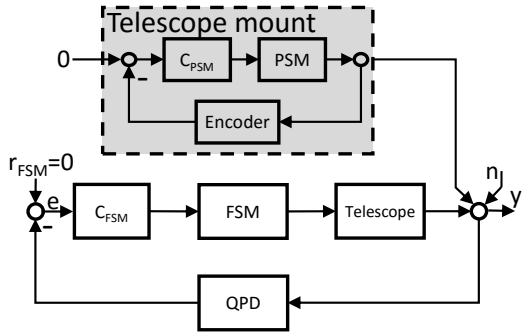

Fig. 6. Block diagram for one axis of the proposed QPD based feedback controller (C_{FSM}) driving the FSM, where n is the output disturbance. The mount is used with static reference input in this configuration.

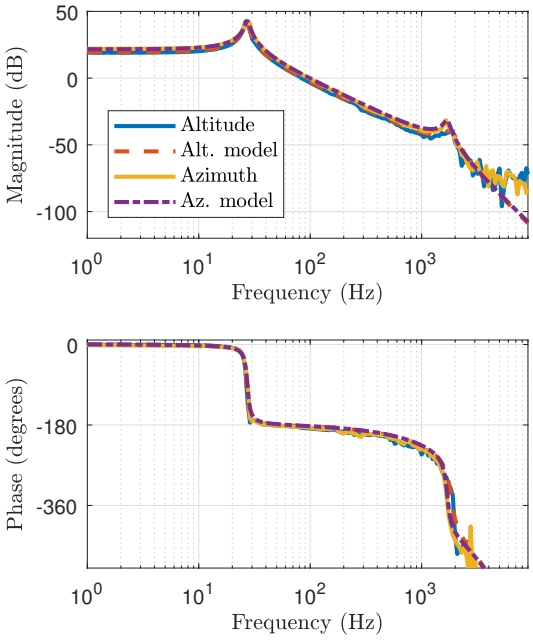

Fig. 7. Measured frequency response of the FSM plant consisting of the amplifier, FSM and QPD (solid). Two spring-damper-mass system models are fitted manually for each axis (dashed).

The frequency response of the mirror is modeled by a pair of second order transfer functions, one modeling the contributions of the first mode of the mirror at 27 Hz and the second transfer function representing the behavior of the second mode at 1850 Hz (alt) and 1700 Hz (az). Additionally a dead time accounts for the delay due to the sampling system (f_s = 18 kHz). The frequency response of these models is shown in Figure 7. A small offset in the magnitude plot between the two axes is caused by gain variations of the QPD. The mirror itself is designed and built symmetrically.

According to Csencsics and Schitter (2017) the first structural mode of the mirror is located at 850 Hz (not observable by the QPD) and is considered as an upper bandwidth limit for imaging applications, as the reflection of the mirror surface may degrade at higher frequencies. Again an independent SISO controller is used for each axis. The previously derived feedback controllers based on the mount as presented in Subsection 3.1, are disabled, when the FSM based controllers are used. Therefor, no stability issues may arise due to interactions between both control loops. Tamed PID controllers (Equation 1) are designed based on the open loop plant model [Munning Schmidt et al. (2014)]. Similar to the controllers used for the mount, their transfer function is given by

$$C_{\mathrm{FSM}}(s) = K_p + \frac{K_i}{s} + \frac{K_d s}{\tau_t s + 1}. \tag{2}$$

The unity-gain crossover frequency is set to 330 Hz for the alt axis and 320 Hz for the azimuth axis, achieving a phase margin of 37° and a gain margin of 10 dB. The crossover frequency is selected to achieve maximum bandwidth but with phase and gain margins comparable to the mount controller's. This results in a closed loop bandwidth of 772 Hz (alt) and 810 Hz (az).

Figure 8 depicts the measured sensitivity functions for the FSM based closed loop system, showing similar behavior for both axes. It was measured from the reference input of the controller to the error signal of the same controller. The 0 dB line is crossed at approximately 240 Hz. A significant rejection of vibrations for frequencies below 100 Hz is visible. Peaking is present from 110 Hz to 1 kHz, due to the waterbed effect. For the application of vibration compensation the significant disturbance rejection in the low frequency range outweighs the resulting disturbance amplification by the waterbed effect Munning Schmidt et al. (2014).

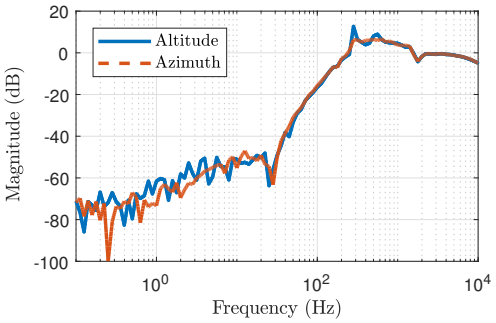

Fig. 8. Measured sensitivity functions of the FSM based closed loop system. Both cross the 0 dB line at approximately 240 Hz.

Pre-print version of the article: A. Sinn, T. Riel, F. Deisl, S. Schachner, and G. Schitter, "High-bandwidth tip-tilt vibration compensation in telescope systems," *Joint Conference 8th IFAC Symposium on Mechatronic Systems (MECHATRONICS 2019)*, vol. 52, no. 15, pp. 549 – 554, 2019. DOI: 10.1016/j.ifacol.2019.11.733
© 2019. This manuscript version is made available under the CC-BY-NC-ND 4.0 license
http://creativecommons.org/licenses/by-nc-nd/4.0/

Pre-print version (generated on 15.12.2021)
This and other publications are available at:
http://www.acin.tuwien.ac.at/publikationen/ams/

4. EXPERIMENTAL RESULTS

The designed controllers are implemented on a dSpace rapid prototyping system and the setup's performance is evaluated in a laboratory environment. To characterize the (vibration-)disturbance rejection capability of the compensation system, a disturbance profile meeting the spectral BBN VC-A criterion [Ungar and Gordon (1983)] is applied to the reference input of the designed controllers. This disturbance signal does not only account for ground vibrations, but also for wind shake induced disturbances. Measurement output is the error signal of the same controller, resulting in a transfer function, which is equivalent to the output-disturbance to output transfer function. A system analyzer is used to record the frequency responses, as well as the power spectral densities (PSDs).

To allow the comparison of both proposed control loops against a neutral reference, a measurement series without external (QPD based) feedback is performed. The disturbance profile is applied to the reference input of the mount. In this case the telescope quasi-statically points at the artificial star without external feedback, thus having only position control based on the internal encoders of the mount. The output of the QPD is recorded and plotted labeled as "Reference".

The performance of the two compensation loops is compared to the reference system in the frequency domain. The PSDs of the measured tip-tilt errors is shown in Figure 9 for the alt-axis and in Figure 10 for the az-axis. Due to the limited bandwidth of the compensation system based on the mount, tip-tilt errors are only reduced significantly in the frequency range below approximately 1 Hz (alt) and 0.4 Hz (az). The peak at 10.6 Hz visible in both reference and mount controlled PSDs is caused by an eigenmode of the supporting workbench. The FSM based system increases the compensation bandwidth by a factor of approximately 100.

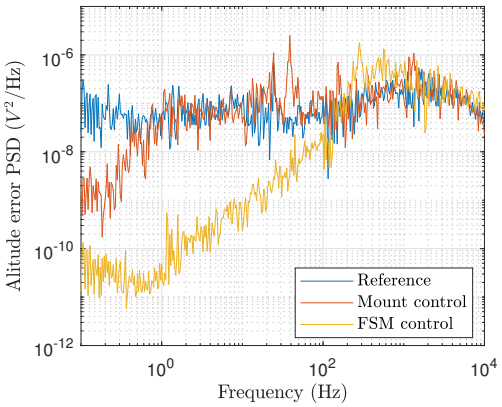

Fig. 9. Measured PSDs of the QPD output of the altitude axis. The reference signal (blue) is measured without external feedback from the QPD. It is compared the the performance feedback control based on the QPD and the mount as actuator (orange), as well as the FSM as actuator (yellow).

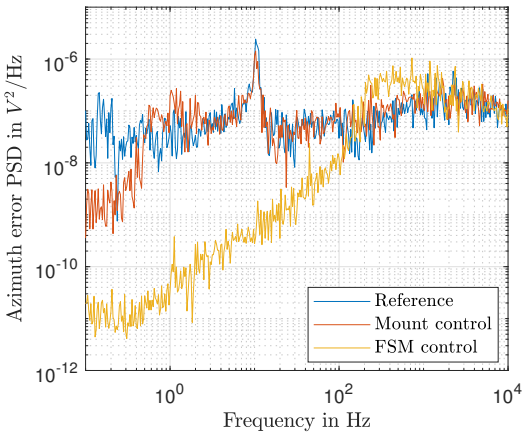

Fig. 10. Measured PSDs of the QPD output of the azimuth axis. The reference signal (blue) includes no external feedback by the QPD. The compensation system using the mount (orange) contributes below 0.4 Hz. The FSM based system (yellow) shows a significantly higher compensation bandwidth of about 100 Hz.

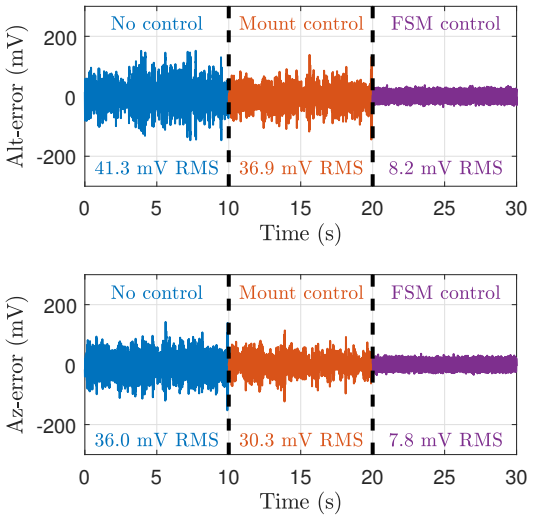

Fig. 11. Measured tip-tilt error signals. In the beginning no QPD based control is applied (mean values are removed for comparison). At 10 s the feedback loop using the mount is closed. At 20 s this loop is inactivated, and the FSM control loop is closed. In comparison to the original system, the FSM based tip-tilt compensation system reduces the RMS error by a factor of 5 (alt) and a factor of 4.6 (az).

Figure 11 compares the measured time signals of the reference system to the mount based, as well as the FSM based control loops. Transients which may occur during switching between control loops are removed, to allow direct comparison of the performance of the systems. Starting at time zero a measurement of 10 s duration

Pre-print version of the article: A. Sinn, T. Riel, F. Deisl, S. Schachner, and G. Schitter, "High-bandwidth tip-tilt vibration compensation in telescope systems," *Joint Conference 8th IFAC Symposium on Mechatronic Systems (MECHATRONICS 2019),* vol. 52, no. 15, pp. 549 – 554, 2019. DOI: 10.1016/j.ifacol.2019.11.733
© 2019. This manuscript version is made available under the CC-BY-NC-ND 4.0 license
http://creativecommons.org/licenses/by-nc-nd/4.0/

Pre-print version (generated on 15.12.2021)
This and other publications are available at:
http://www.acin.tuwien.ac.at/publikationen/ams/

quantifies the influence of vibrations to the reference system. Its mean value caused by minimal deviations of the focused spot from the artificial start on the QPD is subtracted for the purpose of comparability. After 10 seconds feedback control based on the QPD measurement and the telescope mount is enabled, reducing the RMS tip-tilt error by 11 % (altitude) and 16 % (azimuth). After 20 seconds the loop based on the mount is disabled and the FSM based control loop is closed, resulting in an reduction of the RMS tip-tilt error by a factor of 5 in the altitude and a factor of 4.6 in the azimuth axis.

In summary, the QPD-based feedback control for telescope systems is able to significantly reduce the impact of vibrations. Using the telescope mount for compensation a reduction by up to 15 %, and using the FSM a reduction by a factor of up to 5 is achieved.

5. CONCLUSION

In this paper a high-bandwidth tip-tilt vibration compensation system for telescope systems based on absolute position information from a quad photo diode (QPD) is investigated. The system implements feedback control using a fast steering mirror (FSM) and the sensor information from the QPD and is evaluated under laboratory conditions. This control loop is compared to a loop based on the same QPD and the telescope mount as compensation actuator. The comparison of both systems to the original system without external position feedback shows a reduction of up to 15 % for the control loop using the telescope mount and a reduction by a factor of up to 5 for the FSM system, successfully demonstrating the potential of this compensation strategy.

ACKNOWLEDGEMENTS

The authors gratefully acknowledge the excellent cooperation with ASA Astrosysteme GmbH and thank for its support and valuable expertise.

REFERENCES

Bely, P.Y. (2003). *The Design and Construction of Large Optical Telescopes*. Springer.

Csencsics, E. and Schitter, G. (2017). System Design and Control of a Resonant Fast Steering Mirror for Lissajous-Based Scanning. *IEEE/ASME Transactions on Mechatronics*, 22(5), 1963–1972.

Glück, M., Pott, J.U., and Sawodny, O. (2017). Investigations of an accelerometer-based disturbance feedforward control for vibration suppression in adaptive optics of large telescopes. *Publications of the Astronomical Society of the Pacific*, 129(976), 65001.

Hardy, J.W. (1998). *Adaptive optics for astronomical telescopes*. Oxford University Press, New York.

Hemmati, H. (2007). Interplanetary Laser Communications. *Optics and Photonics*, 18, 22–27.

Jim, K.T., Pickles, A.J., Yamada, H.T., Graves, J.E., Stockton, A., Northcott, M.J., Young, T., Cowie, L.L., Luppino, G.A., Thornton, R.J., Kupke, R., Sousa, E., Cavedoni, C.P., Keller, T.J., Nakamura, W., and Metzger, M.R. (2000). The University of Hawaii 2.2 Meter Fast Tip-Tilt Secondary System. *Publications of the Astronomical Society of the Pacific*, 112, 716–732.

Kaymak, Y., Rojas-Cessa, R., Feng, J.H., Ansari, N., Zhou, M.C., and Zhang, T. (2018). A Survey on Acquisition, Tracking, and Pointing Mechanisms for Mobile Free-Space Optical Communications. *IEEE Communications Surveys and Tutorials*, 20(2), 1104–1123. doi:10.1109/COMST.2018.2804323.

Keck, A., Pott, J.U., and Sawodny, O. (2014). Accelerometer-based online reconstruction of vibrations in extremely large telescopes. In *19th World Congress IFAC*, 7467–7473.

Lee, S., Ortiz, G.G., Alexander, J.W., Portillo, A., and Jeppesen, C. (2001). Accelerometer-assisted tracking and pointing for deep space optical communications. In *IEEE Aerospace Conference Proceedings*, 1559–1564.

Munning Schmidt, R., Schitter, G., Rankers, A., and Van Eijk, J. (2014). *The Design of High Performance Mechatronics*. Delft University Press, Amsterdam, 2nd edition.

Peter, D., Gässler, W., Borelli, J., Barl, L., and Rabien, S. (2012). Vibration control for the ARGOS laser launch path. 8447, 84474J–84474J–8.

Pickles, A.J., Young, T.T., Nakamura, W., Cowie, L.L., Graves, J.E., Jim, K.T.C., Keller, T.J., Luppino, G.A., Northcott, M.J., Roddier, C.A., Stockton, A.N., Wainscoat, R.J., Yamada, H., and Cavedoni, C.P. (1994). UH/IfA fast tip-tilt secondary. In *Symposium on Astronomical Telescopes & Instrumentation for the 21st Century*, June 1994, 504–515.

Riel, T., Galffy, A., Sinn, A., and Schitter, G. (2017). Improvement of the angular precision of anoptical metrology platform by disturbance compensation. In *Proceedings of ASPE Spring Topical Meeting - Precision Engineering and Optics: What are the Limits of Precision, and How to Characterize Them?*, 15–20.

Riel, T., Galffy, A., and Schitter, G. (2018a). Analysis and robust control of an precision motion platform using disturbance compensation. In *IEEE Conference on Control Technology and Applications*, 1090–1095.

Riel, T., Saathof, R., Katalenic, A., Ito, S., and Schitter, G. (2018b). Noise analysis and efficiency improvement of a pulse-width modulated permanent magnet synchronous motor by dynamic error budgeting. *Mechatronics*, 50, 225–233.

Riesing, K., Yoon, H., and Cahoy, K. (2017). A portable optical ground station for low-earth orbit satellite communications. In *Proc. of IEEE International Conference on Space Optical Systems and Applications*, 118–124.

Schmidt, C. (2012). Wide-field-of-regard pointing, acquisition and tracking-system for small laser communication terminals. *Proc. International Conference on Space Optical Systems and Applications*, 12, 4–9.

Sinn, A., Riel, T., Kremsner, P., and Schitter, G. (2019). Analysis of tip-tilt compensation for reflective free-space optical satellite communication. In *Proc. of SPIE Vol. 10910*, 109101G–1 – 109101G–12.

Ungar, E. and Gordon, C. (1983). Vibration criteria for microelectronics manufacturing equipment. In *Proceedings of International Conference on Noise Control Engineering*, 487–490.

Yamaguchi, T., Hirata, M., and Pang, C.K. (2011). *High-Speed Precision Motion Control*. CRC Press, Boca Raton.

Pre-print version of the article: A. Sinn, T. Riel, F. Deisl, S. Schachner, and G. Schitter, "High-bandwidth tip-tilt vibration compensation in telescope systems," *Joint Conference 8th IFAC Symposium on Mechatronic Systems (MECHATRONICS 2019),* vol. 52, no. 15, pp. 549 – 554, 2019. DOI: 10.1016/j.ifacol.2019.11.733
© 2019. This manuscript version is made available under the CC-BY-NC-ND 4.0 license
http://creativecommons.org/licenses/by-nc-nd/4.0/